PREPRINT: Annual Conf. Inf. Fusion, Salamanca, Spain, July 2014

Multi-Object Tracking Using Labeled Multi-Bernoulli Random Finite Sets

Stephan Reuter*, Ba-Tuong Vo†, Ba-Ngu Vo†, Klaus Dietmayer*
* Institute of Measurement, Control and Microtechnology
Ulm University, Ulm, Germany,
{stephan.reuter, klaus.dietmayer}@uni-ulm.de.
† Department of Electrical and Computer Engineering
Curtin University, Bentley, Australia
{ba-tuong.vo, ba-ngu.vo}@curtin.edu.au

***Abstract*—In this paper, we propose the labeled multi-Bernoulli filter which explicitly estimates target tracks and provides a more accurate approximation of the multi-object Bayes update than the multi-Bernoulli filter. In particular, the labeled multi-Bernoulli filter is not prone to the biased cardinality estimate of the multi-Bernoulli filter. The utilization of the class of labeled random finite sets naturally incorporates the estimation of a targets identity or label. Compared to the δ-generalized labeled multi-Bernoulli filter, the labeled multi-Bernoulli filter is an efficient approximation which obtains almost the same accuracy at significantly lower computational cost. The performance of the labeled multi-Bernoulli filter is compared to the multi-Bernoulli filter using simulated data. Further, the real-time capability of the filter is illustrated using real-world sensor data of our experimental vehicle.**

Keywords*—Random finite set, labeled multi-Bernoulli, Bayesian estimation, target tracking.

I. Introduction

The aim of multi-object tracking is to jointly estimate the number of objects and their states using a sequence of measurements. Multi-object tracking is much more challenging than single-object tracking due to object births and deaths [1], [2], [3]. Further, the measurement process is prone to missed detections and false alarms which typically leads to ambiguities in the track to measurement association. During the last decades, Multiple Hypotheses Tracking (MHT) [1] and Joint Probabilistic Data Association (JPDA) [2] have been extensively used in a variety of multi-object tracking applications. Within the random finite set approach to multi-object tracking [3], the multi-object state is represented as a random finite set (RFS) which naturally captures the uncertainty in the number of objects as well as in the individual object states. Finite set statistics facilitate the derivation of the multi-object Bayes filter [3] which recursively propagates the multi-object posterior density in time.

The computational complexity of the multi-object Bayes filter induced the development of several approximations. The Probability Hypothesis Density (PHD) [4] filter and the Cardinalized PHD (CPHD) [5] filter approximate the recursion by propagating the first moment and the cardinality distribution of the multi-object posterior density over time. In contrast, the multi-Bernoulli filters proposed in [6], [7] propagate the parameters of a multi-Bernoulli distribution over time. Implementations of the filters using Gaussian mixture (GM) and sequential Monte Carlo (SMC) methods are presented in [6], [8], [9], [10], [11], [12].

The multi-Bernoulli approximations of the multi-object Bayes filter are suitable for tracking applications which require object individual existence probabilities or particle implementations. While the particle implementations of the PHD and CPHD filters require error-prone track extraction algorithms, the multi-Bernoulli representation facilitates a straightforward extraction of the objects' states. Several extensions of the multi-Bernoulli filter are proposed in [13], [14], [15], [16]. Applications of the multi-Bernoulli filter include visual tracking and cell tracking [17], [18], tracking in sensor networks [19], [20], as well as multi-sensor tracking using video and audio data [21]. Further, a hybrid multi-Bernoulli and Poisson multi-object tracking filter is proposed in [22].

This paper proposes a novel multi-object tracking algorithm, the labeled multi-Bernoulli (LMB) filter. While the approximations within the derivation of the multi-Bernoulli filter require a high detection probability and a low false alarm rate, the LMB filter does not depend on these restrictions. However, the LMB filter also provides the advantages of the multi-Bernoulli filter including particle implementations and straightforward state estimation. Additionally, the proposed LMB filter estimates target tracks by utilizing the class of labeled RFSs [23], [24]. Compared to the δ-generalized labeled multi-Bernoulli filter [24], the LMB filter represents an efficient approximation which significantly reduces the computational complexity due to a dynamic grouping procedure. Compared to the multi-Bernoulli filter, the LMB filter achieves superior performance at the cost of an increased computational complexity. The proposed filter is compared to the multi-Bernoulli filter using simulated data. Additionally, the real-time capability is illustrated using real-world sensor data for typical scenarios in vehicle environment perception.

This paper is organized as follows: First, the class of labeled random finite sets is reviewed. In Section III, the labeled multi-Bernoulli filter is proposed. Afterwards, the implementation of the filter using grouping and gating is explained in detail. Finally, tracking results using simulated as well as real world sensor data are presented in Section V.

TABLE I. NOTATION

- small letters (e.g. x) denote single-object states.
- capital letters (e.g. X) denote multi-object states.
- labeled distributions and states (e.g. $\boldsymbol{\pi}$, $\mathbf{x}$, $\mathbf{X}$) are indicated by bold face letters.
- spaces are represented by blackboard bold letters, e.g. $\mathbb{X}$ denotes the state space and $\mathbb{Z}$ denotes the measurement space.
- finite subsets of $\mathbb{X}$ are denoted by $\mathcal{F}(\mathbb{X})$. All finite subsets comprising n elements are denoted by$\mathcal{F}_n(\mathbb{X})$.
- the inner product of two functions $f(x)$ and $g(x)$ is abbreviated by
$$\langle f, g \rangle \triangleq \int f(x)g(x)dx.$$
- the multi-object exponential notation for a real-valued function h is given by
$$h^X \triangleq \prod_{x \in X} h(x),$$
where $h^{\emptyset} = 1$.
- the generalized Kronecker delta function which supports sets, vectors and integers is given by
$$\delta_Y(X) \triangleq \begin{cases} 1, \text{ if } X = Y \\ 0, \text{ otherwise.} \end{cases}$$
- the inclusion function is defined by
$$1_Y(X) \triangleq \begin{cases} 1, \text{ if } X \subseteq Y \\ 0, \text{ otherwise} \end{cases}$$
and $1_Y(\{x\})$ is abbreviated by $1_Y(x)$ if X is a singleton.

II. LABELED RANDOM FINITE SETS

This section reviews the class of labeled random finite sets introduced in [24] and provides the required details for the labeled multi-Bernoulli (LMB) and the δ-generalized labeled multi-Bernoulli (δ-GLMB) RFS. For additional details and other labeled multi-object distributions (e.g. labeled Poisson RFS), the reader is referred to [23], [24] and [25]. Table I summarizes several notations used throughout this paper.

In order to enable the estimation of an objects trajectory in multi-object scenarios, a label $\ell \in \mathbb{L}$ is appended to the state $x \in \mathbb{X}$. In general, the labels ℓ are elements of a discrete label space $\mathbb{L}= \{\alpha_i : i \in \mathbb{N}\}$, whose elements α_i are distinct. Further, the space $\mathbb{N}$ denotes the set of positive integers. In multi-object tracking applications, the labels of a multi-object state X are required to be unique, i.e. each object $x \in X$ is augmented by a distinct label. Thus, a labeled RFS [24] is a finite set valued random variable on the space $\mathbb{X}\times\mathbb{L}$ where all realizations of the label space contain unique labels.

As introduced in [25], a label $\ell = (k, i)$ is assigned to each object which is a pair of the time of birth k and a unique index $i \in \mathbb{N}$. Thus, the labeled state space of a new born objects at time k is given by $\mathbb{L}_k = k \times \mathbb{N}$. The label space for all objects born before time k is $\mathbb{L}_{0:k-1}$. Since the label sets for new born and already existing objects are disjoint, the label space for all objects at time k is $\mathbb{L}_{0:k} = \mathbb{L}_{0:k-1} \cup \mathbb{L}_k$. For notational convenience, the following abbreviations are used: $\mathbb{L} = \mathbb{L}_{0:k}$, $\mathbb{B} = \mathbb{L}_{k+1}$, $\mathbb{L}_+ = \mathbb{L} \cup \mathbb{B}$. Further, the labels of the objects are static.

For a realization of a labeled RFS $\mathbf{X}$, the set of labels is given by $\mathcal{L}(\mathbf{X}) = \{\mathcal{L}(\mathbf{x}) : \mathbf{x} \in \mathbf{X}\}$, where $\mathcal{L}((x, \ell)) = \ell$ represents the projection from the labeled state space to the label space. Since the labels of a realization $\mathbf{X}$ of a labeled RFS are required to be distinct, the cardinalities of the set of labels and the set of state vectors have to be equivalent, i.e. $|\mathcal{L}(\mathbf{X})| = |\mathbf{X}|$, which is ensured using the distinct label indicator

$$\Delta(\mathbf{X}) = \delta_{|\mathbf{X}|}(|\mathcal{L}(\mathbf{X})|). \tag{1}$$

The unlabeled version of a labeled RFS on the space $\mathbb{X} \times \mathbb{L}$ is given by the projection to the state space $\mathbb{X}$ [24] using marginalization. Further, the cardinality distribution of a labeled RFS matches the one of its unlabeled version.

A. Labeled Multi-Bernoulli RFS

The density of a labeled multi-Bernoulli (LMB) RFS with state space $\mathbb{X}$ and label space $\mathbb{L}$ is given by [24]

$$\boldsymbol{\pi}\left(\{(x_1, \ell_1), ..., (x_n, \ell_n)\}\right) = \delta_n(|\{\ell_1, ...\ell_n\}|) \prod_{\zeta \in \Psi} \left(1 - r^{(\zeta)}\right) \times \prod_{j=1}^{n} \frac{1_{\alpha(\Psi)}(\ell_j) r^{(\alpha^{-1}(\ell_j))} p^{(\alpha^{-1}(\ell_j))}(x_j)}{1 - r^{(\alpha^{-1}(\ell_j))}}. \tag{2}$$

Similar to a multi-Bernoulli RFS [3], [6], an LMB RFS is completely described by the parameter set $\{(r^{(\zeta)}, p^{(\zeta)}) : \zeta \in \Psi\}$ with index set Ψ since the components ζ are assumed to be statistically independent. In the following, the density of an LMB RFS is abbreviated by its parameter set.

For notational convenience, the mapping α is assumed to be an identity mapping, i.e. the component indices correspond to the label of the track. An alternative representation of the LMB density with parameter set $\boldsymbol{\pi} = \{r^{(\ell)}, p^{(\ell)}\}_{\ell \in \mathbb{L}}$ is given by

$$\boldsymbol{\pi}(\mathbf{X}) = \Delta(\mathbf{X}) w(\mathcal{L}(\mathbf{X})) p^{\mathbf{X}} \tag{3}$$

where

$$w(L) = \prod_{i \in \mathbb{L}} \left(1 - r^{(i)}\right) \prod_{\ell \in L} \frac{1_{\mathbb{L}}(\ell) r^{(\ell)}}{1 - r^{(\ell)}}, \tag{4}$$

$$p(x, \ell) = p^{(\ell)}(x). \tag{5}$$

Further, the cardinality distribution of an LMB RFS yields

$$\boldsymbol{\rho}(n) = \prod_{i \in \mathbb{L}} \left(1 - r^{(i)}\right) \cdot \sum_{L \in \mathcal{F}_n(\mathbb{L})} \prod_{\ell \in L} \frac{r^{(\ell)}}{1 - r^{(\ell)}} \tag{6}$$

and the PHD of its unlabeled version is given by

$$v(x) = \sum_{i \in \mathbb{L}} r^{(i)} p^{(i)}(x). \tag{7}$$

B. δ-Generalized Labeled Multi-Bernoulli RFS

The density of a δ-generalized labeled multi-Bernoulli (δ-GLMB) RFS [24] with state space $\mathbb{X}$ and label space $\mathbb{L}$ is given by

$$\boldsymbol{\pi}(\mathbf{X}) = \Delta(\mathbf{X}) \sum_{(I,\xi) \in \mathcal{F}(\mathbb{L}) \times \Xi} w^{(I,\xi)} \delta_I(\mathcal{L}(\mathbf{X})) \left[p^{(\xi)}\right]^{\mathbf{X}}, \tag{8}$$

where I represents a set of track labels and ξ denotes a realization of a discrete space Ξ. In the context of multi-object tracking applications, the realizations of the discrete space Ξ denote the history of track label to measurement associations [24]. The joint label set and discrete index pairs (I, ξ) are referred to as a "hypothesis" in the following. Thus, a δ-GLMB

RFS is able to represent several association hypotheses for a set of track labels I and facilitates the derivation of the δ-GLMB filter.

An LMB RFS on the space $\mathbb{X}\times\mathbb{L}$ with parameter set $\boldsymbol{\pi} = \{r^{(\ell)}, p^{(\ell)}\}_{\ell\in\mathbb{L}}$ is a special case of a δ-GLMB RFS. Since the tracks $\ell \in \mathbb{L}$ of an LMB RFS are statistically independent, an LMB RFS does not facilitate multiple hypotheses for a set of track labels I which corresponds to setting $\Xi = \emptyset$. Thus, (8) simplifies to

$$\boldsymbol{\pi}(\mathbf{X}) = \Delta(\mathbf{X})w(\mathcal{L}(\mathbf{X}))p^{\mathbf{X}} \tag{9}$$

since there is only a single feasible set $I = \mathcal{L}(\mathbf{X})$. Comparing (9) with (3), (9) denotes an LMB RFS if the weights $w(\mathcal{L}(\mathbf{X}))$ follow the multi-Bernoulli distribution (4).

The PHD of the unlabeled version of a δ-GLMB RFS is given by

$$\begin{aligned} v(x) &= \sum_{(I,\xi)\in\mathcal{F}(\mathbb{L})\times\Xi} \sum_{\ell\in\mathbb{L}} p^{(\xi)}(x,\ell) \sum_{L\subseteq\mathbb{L}} 1_L(\ell) w^{(I,\xi)} \delta_I(L) \\ &= \sum_{\ell\in\mathbb{L}} \sum_{(I,\xi)\in\mathcal{F}(\mathbb{L})\times\Xi} w^{(I,\xi)} 1_I(\ell) p^{(\xi)}(x,\ell). \end{aligned} \tag{10}$$

where the inclusion function $1_I(\ell)$ ensures that the summands of the inner sum are zero for all sets of track labels which do not include the track ℓ. Consequently, the PHD of track ℓ is represented by the inner sum in (10), i.e.

$$v^{(\ell)}(x) = \sum_{(I,\xi)\in\mathcal{F}(\mathbb{L})\times\Xi} w^{(I,\xi)} 1_I(\ell) p^{(\xi)}(x,\ell), \tag{11}$$

and its existence probability is obtained by

$$r^{(\ell)} = \sum_{(I,\xi)\in\mathcal{F}(\mathbb{L})\times\Xi} w^{(I,\xi)} 1_I(\ell).$$

Using the PHD and the existence probability, the spatial distribution of track ℓ is given

$$p^{(\ell)} = \frac{v^{(\ell)}(x)}{r^{(\ell)}}. \tag{12}$$

The spatial distribution $p^{(\ell)}$ and the existence probability $r^{(\ell)}$ obtained by the PHD facilitate the approximation of a δ-GLMB RFS using an LMB RFS with parameter set $\boldsymbol{\pi} = \{r^{(\ell)}, p^{(\ell)}\}_{\ell\in\mathbb{L}}$. The LMB approximation matches the PHD of the δ-GLMB RFS, i.e. the spatial distribution of the individual tracks ℓ and the mean cardinalities are identical. However, the approximation loses information about the cardinality distribution. While the cardinality distribution of a δ-GLMB RFS follows

$$\begin{aligned} \boldsymbol{\rho}(n) &= \sum_{(I,\xi)\in\mathcal{F}(\mathbb{L})\times\Xi} \sum_{L\in\mathcal{F}_n(\mathbb{L})} w^{(I,\xi)} \delta_I(L) \\ &= \sum_{(I,\xi)\in\mathcal{F}_n(\mathbb{L})\times\Xi} w^{(I,\xi)} \end{aligned} \tag{13}$$

which facilitates arbitrary (e.g. multi-modal) distributions, the cardinality distribution of an LMB RFS is restricted to a multi-Bernoulli distribution which is uni-modal.

III. The Labeled Multi-Bernoulli Filter

The labeled multi-Bernoulli (LMB) filter approximates the predicted and posterior multi-object densities within the multi-object Bayes filter [3] as a labeled multi-Bernoulli process which represents each track by an existence probability r and the according spatial distribution $p(x)$. The derivation of LMB filter utilizes the result that a δ-GLMB RFS is closed under the multi-target prediction and update operations [24].

Compared to the δ-GLMB filter [24], the proposed LMB filter requires a significantly smaller number of components. While the number of hypotheses (I,ξ) of the δ-GLMB filter grows exponentially in the number of objects, the number of tracks within the LMB filter increases linearly. Compared to the multi-Bernoulli filter proposed in [6], the LMB approximation is more accurate since it only requires the approximation of the posterior δ-GLMB RFS by an LMB RFS with matching PHD. In contrast, the multi-Bernoulli filter involves two approximations of the probability generating functional of the multi-object posterior which additionally require a high detection probability and a reasonably small false alarm rate.

In the following, the exact time prediction step as well as the approximate measurement update are derived. For notational convenience, the time indices of predicted values are abbreviated by a "+" (e.g. $X_+ \triangleq X_{k+1|k}$) and the ones of posterior values are omitted.

A. Prediction

Proposition 1: Assume that the prior density is an LMB RFS with state space $\mathbb{X}$, (finite) label space $\mathbb{L}$, and parameter set $\boldsymbol{\pi} = \{r^{(\ell)}, p^{(\ell)}\}_{\ell\in\mathbb{L}}$ and the birth density is an LMB RFS with state space $\mathbb{X}$, label space $\mathbb{B}$, and parameter set $\boldsymbol{\pi}_B = \{r_B^{(\ell)}, p_B^{(\ell)}\}_{\ell\in\mathbb{B}}$, i.e.

$$\boldsymbol{\pi}(\mathbf{X}) = \Delta(\mathbf{X})w(\mathcal{L}(\mathbf{X}))p^{\mathbf{X}} \tag{14}$$

$$\boldsymbol{\pi}_B(\mathbf{X}) = \Delta(\mathbf{X})w_B(\mathcal{L}(\mathbf{X}))\left[p_B\right]^{\mathbf{X}} \tag{15}$$

with

$$w(L) = \prod_{i\in\mathbb{L}} \left(1 - r^{(i)}\right) \prod_{\ell\in L} \frac{1_{\mathbb{L}}(\ell) r^{(\ell)}}{1 - r^{(\ell)}}, \tag{16}$$

$$w_B(L) = \prod_{i\in\mathbb{B}} \left(1 - r_B^{(i)}\right) \prod_{\ell\in L} \frac{1_{\mathbb{B}}(\ell) r_B^{(\ell)}}{1 - r_B^{(\ell)}}, \tag{17}$$

$$p(x,\ell) = p^{(\ell)}(x), \tag{18}$$

$$p_B(x,\ell) = p_B^{(\ell)}(x), \tag{19}$$

where the label spaces of existing and new born objects are distinct, i.e. $\mathbb{L}\cap\mathbb{B} = \emptyset$. Then, the predicted LMB density with state space $\mathbb{X}$ and label space $\mathbb{L}_+ = \mathbb{B}\cup\mathbb{L}$ is given by the parameter set

$$\boldsymbol{\pi}_+ = \left\{\left(r_{+,S}^{(\ell)}, p_{+,S}^{(\ell)}\right)\right\}_{\ell\in\mathbb{L}} \cup \left\{\left(r_B^{(\ell)}, p_B^{(\ell)}\right)\right\}_{\ell\in\mathbb{B}}, \tag{20}$$

where

$$r_{+,S}^{(\ell)} = \eta_S(\ell) r^{(\ell)}, \tag{21}$$

$$p_{+,S}^{(\ell)} = \left\langle p_S(\cdot,\ell) f(x|\cdot,\ell), p(\cdot,\ell)\right\rangle / \eta_S(\ell), \tag{22}$$

$$\eta_S(\ell) = \left\langle p_S(\cdot,\ell), p(\cdot,\ell)\right\rangle, \tag{23}$$

and $p_S(\cdot,\ell)$ denotes the state dependent persistence probability of track ℓ. Further, $f(x|\cdot,\ell)$ is the single-object Markov transition density.

In [24], the δ-GLMB RFS is shown to be closed under the prediction step although the number of components increases

exponentially. Since an LMB RFS is a special case of a δ-GLMB RFS, the posterior LMB RFS may be rewritten in δ-GLMB form. Consequently, the prediction of an LMB RFS follows a δ-GLMB RFS. However, the weights of the predicted δ-GLMB RFS follow a multi-Bernoulli distribution and the predicted δ-GLMB RFS actually coincides with the LMB RFS given by (20). Thus, an LMB RFS is closed under the prediction. A detailed proof of the proposition using induction is given in [26].

It turns out, that the prediction of an LMB RFS is identical to the prediction of the unlabeled multi-Bernoulli distribution within the CB-MeMBer filter [6]. Hence, the implementation of the LMB filter prediction is given by the GM and SMC equations of the CB-MeMBer filter proposed in [6].

B. Update

In contrast to the prediction step, an LMB RFS is not closed under the multi-target Bayes update. Since the δ-GLMB RFS is shown in [24] to be closed under the update operation, the measurement update of an LMB RFS is again a δ-GLMB RFS. As introduced in Section II-B, the PHD facilitates the approximation of a δ-GLMB RFS by an LMB RFS which exactly matches the first moment of the δ-GLMB RFS.

Proposition 2: Assume that the predicted LMB RFS with state space $\mathbb{X}$ and label space $\mathbb{L}_+$ is given by the parameter set

$$\boldsymbol{\pi}_+ = \left\{ (r_+^{(\ell)}, p_+^{(\ell)}) \right\}_{\ell \in \mathbb{L}_+}. \tag{24}$$

Then, the LMB RFS with state space $\mathbb{X}$, label space $\mathbb{L}_+$, and parameter set

$$\boldsymbol{\pi}(\cdot|Z) = \{(r^{(\ell)}, p^{(\ell)}(\cdot))\}_{\ell \in \mathbb{L}_+} \tag{25}$$

where

$$r^{(\ell)} = \sum_{(I_+,\theta) \in \mathcal{F}(\mathbb{L}_+) \times \Theta_{I_+}} w^{(I_+,\theta)}(Z) 1_{I_+}(\ell), \tag{26}$$

$$p^{(\ell)}(x) = \frac{1}{r^{(\ell)}} \sum_{(I_+,\theta) \in \mathcal{F}(\mathbb{L}_+) \times \Theta_{I_+}} w^{(I_+,\theta)}(Z) 1_{I_+}(\ell) p^{(\theta)}(x,\ell) \tag{27}$$

exactly matches the first moment of the unlabeled version of the multi-object posterior. Here, Θ_{I_+} denotes the space of the track label to measurement assignments $\theta : I_+ \to \{0, 1, ..., |Z|\}$, where $\theta(i) = \theta(i') > 0$ implies $i = i'$, and the existence probabilities as well as the spatial distributions of the individual tracks are calculated using

$$w^{(I_+,\theta)}(Z) \propto w_+(I_+)[\eta_Z^{(\theta)}]^{I_+}, \tag{28}$$

$$p^{(\theta)}(x,\ell|Z) = \frac{p_+(x,\ell)\psi_Z(x,\ell;\theta)}{\eta_Z^{(\theta)}(\ell)}, \tag{29}$$

$$\eta_Z^{(\theta)}(\ell) = \langle p_+(\cdot,\ell), \psi_Z(\cdot,\ell;\theta) \rangle, \tag{30}$$

$$\psi_Z(x,\ell;\theta) = \begin{cases} \frac{p_D(x,\ell) g(z_{\theta(\ell)}|x,\ell)}{\kappa(z_{\theta(\ell)})}, & \text{if } \theta(\ell) > 0 \\ q_D(x,\ell), & \text{if } \theta(\ell) = 0 \end{cases}, \tag{31}$$

where $p_D(x,\ell)$ denotes the state dependent detection probability of track ℓ, $q_D(x,\ell) = 1 - p_D(x,\ell)$ is the missed detection probability, $g(z|x,\ell)$ represents the single target measurement likelihood, and $\kappa(\cdot)$ denotes the intensity of the Poisson distributed clutter measurements.

The proof of this proposition is outlined as follows: First, the predicted LMB RFS is equivalently rewritten in δ-GLMB form. Using the δ-GLMB update proposed in [24], the measurement updated parameters given by the equations (28)-(31) are obtained. Note, that the equations are independent of the ξ since the discrete space is $\Xi = \emptyset$. Finally, the parameters $r^{(\ell)}$ and $p^{(\ell)}(x)$ of the posterior LMB RFS are obtained by the approximation of the δ-GLMB RFS using its unlabeled PHD (see Section II-B). Full details of the proof are given in [26].

The proposed LMB approximation only requires the approximation of the multi-object posterior using its first statistical moment. In contrast, the derivation of the CB-MeMBer filter in [6] involves two approximations of the probability generating functional of the multi-object posterior which additionally require a high detection probability and a reasonably low clutter rate. Thus, the proposed LMB filter is more accurate than the CB-MeMBer filter and additionally produces target tracks. Compared to the δ-GLMB filter [24] which represents the posterior using a large sum of multi-target exponentials, the LMB filter requires a significantly smaller amount of components since it approximates the posterior by a set of statistically independent tracks. Due to the approximation, the association uncertainty within the measurement update is represented by the spatial distribution of the individual tracks while the δ-GLMB filter represents all track label to measurement associations using a hypothesis (I, ξ). The PHD approximation within the derivation of the LMB filter results in the loss of information about the cardinality distribution since the cardinality of an LMB RFS follows (6) while the exact cardinality of the posterior is given by (13). However, the matching PHD ensures an identical mean cardinality of the LMB RFS and the full multi-object posterior. Additionally, the spatial distributions of the individual tracks ℓ are identical in both representations.

IV. Implementation of the LMB Filter

At a conceptual level, the proposed LMB filter operates as shown in Figure 1. First, a brief overview of the proposed implementation of the filter is given: The prediction step is performed using a straightforward track by track operation. The LMB representation of the predicted multi-object density facilitates the partitioning into groups using standard gating techniques [2], [27]. Thus, a group only contains closely spaced objects and any measurements which are likely to be associated with them. The grouping allows for parallel group updates and additionally reduces the complexity of each update due to the smaller amount of tracks per group. Each group is updated independently using the LMB filter update proposed in the previous section, i.e. the LMB prediction is converted into the equivalent δ-GLMB form, the standard δ-GLMB update is performed, and the resulting δ-GLMB posterior of each group is approximated by an LMB RFS with matching PHD. Finally, the groups are combined and the track management is applied to the resulting LMB RFS. In the following, the update of the LMB filter is explained in full detail. For details about the GM and SMC implementation of the prediction, refer to [6].

A. Partitioning of Track Labels and Measurements

The representation of the predicted multi-object density in form of an LMB RFS facilitates the partitioning of the

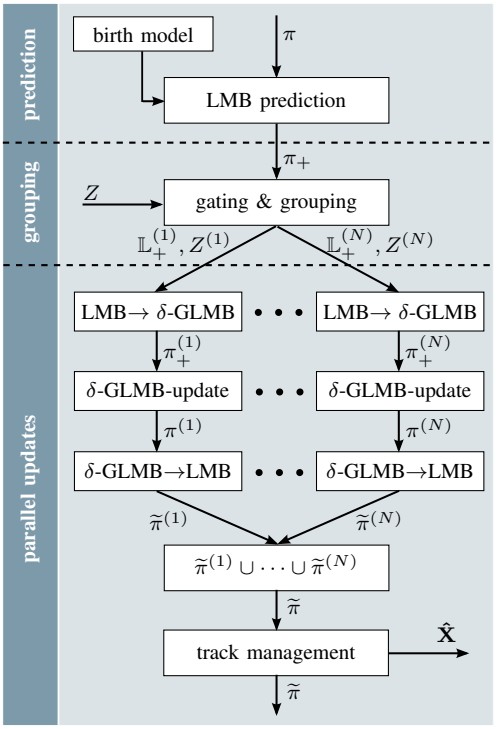

Fig. 1. LMB filter schematic [26].

tracks and measurements into groups. By partitioning the track label subsets with respect to the measurements within the gate, the partitions are well separated and have negligible influence on each other. Obviously, the partitioning requires reasonably small covariances of the birth distributions which are ensured by static birth locations or a measurement driven birth model [26]. The partitioning significantly reduces the computational complexity and provides the possibility of parallel updates at the cost of a small compromise in tracking accuracy.

The grouping procedure partitions the predicted set of track labels using

$$\mathbb{L}_+ = \bigcup_{n=1}^{N} \mathbb{L}_+^{(n)}$$

where $\mathbb{L}_+ = \mathbb{L} \cup \mathbb{B}$ and $\mathbb{L}_+^{(n)} \cap \mathbb{L}_+^{(m)} = \emptyset$ for $n \neq m$. The track label partitions are determined using the spatial distance of the measurements. Thus, partitioning of the measurements results in the mutually exclusive subsets

$$Z = Z^{(0)} \cup \bigcup_{n=1}^{N} Z^{(n)}$$

where the set of measurements $Z^{(n)}$ is associated to the tracks with labels $\mathbb{L}_+^{(n)}$, the measurements in the set $Z^{(0)}$ are assumed to be false alarms, and $Z^{(n)} \cap Z^{(m)} = \emptyset$ if $n \neq m$.

Finally, a pair consisting of a subset of track labels $\mathbb{L}_+^{(n)} \subseteq \mathbb{L}_+$ and the corresponding subset of measurements $Z^{(n)} \subseteq Z$ represents a group

$$\mathcal{G}^{(n)} = \left(\mathbb{L}_+^{(n)}, Z^{(n)}\right). \tag{32}$$

Thus, the predicted LMB RFS can be rewritten by

$$\boldsymbol{\pi}_+ = \bigcup_{i=1}^{N} \boldsymbol{\pi}_+^{(i)} \tag{33}$$

where each group of objects is represented by an LMB RFS

$$\boldsymbol{\pi}_+^{(i)} = \left\{\left(r_+^{(\ell)}, p_+^{(\ell)}\right)\right\}_{\ell \in \mathbb{L}_+^{(i)}}. \tag{34}$$

B. Representation of the Predicted LMB as δ-GLMB

The LMB filter update requires the representation of the predicted LMB RFS in δ-GLMB form to enable the measurement update. Thus, the predicted LMB RFS of each group $\mathcal{G}^{(i)} = (\mathbb{L}_+^{(i)}, Z^{(i)})$ which is given by (34) has to be represented in the equivalent δ-GLMB form

$$\boldsymbol{\pi}_+^{(i)}(\widetilde{\mathbf{X}}_+^{(i)}) = \Delta(\widetilde{\mathbf{X}}_+^{(i)}) \sum_{I_+ \in \mathcal{F}(\mathbb{L}_+^{(i)})} w_{+,i}^{(I_+)} \delta_{I_+}(\mathcal{L}(\widetilde{\mathbf{X}}_+^{(i)}))\, [p_+]^{\widetilde{\mathbf{X}}_+^{(i)}} \tag{35}$$

where

$$w_{+,i}^{(I_+)} = \prod_{\ell \in \mathbb{L}_+^{(i)}} \left(1 - r_+^{(\ell)}\right) \prod_{\ell' \in I_+} \frac{1_{\mathbb{L}_+^{(i)}}(\ell') r_+^{(\ell')}}{1 - r_+^{(\ell')}}. \tag{36}$$

Here, $\widetilde{\mathbf{X}}_+^{(i)}$ denotes the multi-object state of group i. Using the group representation, the required number of hypotheses for the δ-GLMB representation is given by

$$n = \sum_{i=1}^{N} 2^{|\mathbb{L}_+^{(i)}|}. \tag{37}$$

Typically, the number of track labels per group is smaller than $|\mathbb{L}_+|$ which leads to a significantly smaller number of hypotheses for the δ-GLMB representation.

For small sets of track label $\mathbb{L}_+^{(i)}$, the track label hypotheses I_+ for the cardinalities $n = 0, 1, \ldots, |\mathbb{L}_+^{(i)}|$ may be generated in a brute-force way by enumerating the sum in (35). However, the label space $\mathbb{L}_+^{(i)}$ of a group may contain a large number of track labels in case of closely spaced objects which prevents the enumeration. In this case, a truncation of the predicted δ-GLMB RFS to its most significant terms is required. Similar to the prediction step of the δ-GLMB filter, the k most significant terms of (35) may be obtained using the k-shortest paths algorithm [28], [29].

C. δ-GLMB Group Updates

The δ-GLMB update of the predicted multi-object density (35) using the measurement set $Z^{(i)}$ is given by applying the δ-GLMB filter update [24] to each group:

$$\boldsymbol{\pi}^{(i)}(\widetilde{\mathbf{X}}^{(i)}|Z^{(i)}) = \Delta(\widetilde{\mathbf{X}}^{(i)}) \times \sum_{(I_+,\theta) \in \mathcal{F}(\mathbb{L}_+^{(i)}) \times \Theta_{I_+}} w^{(I_+,\theta)}(Z^{(i)}) \delta_{I_+}(\mathcal{L}(\widetilde{\mathbf{X}}^{(i)})) \left[p^{(\theta)}(\cdot|Z^{(i)})\right]^{\widetilde{\mathbf{X}}^{(i)}}. \tag{38}$$

where the weights and the spatial distributions are calculated using

$$w^{(I_+,\theta)}(Z^{(i)}) \propto w_{+,i}^{(I_+)} [\eta_{Z^{(i)}}^{(\theta)}]^{I_+} \tag{39}$$

$$p^{(\theta)}(x,\ell|Z^{(i)}) = \frac{p_+(x,\ell)\psi_{Z^{(i)}}(x,\ell;\theta)}{\eta^{(\theta)}_{Z^{(i)}}(\ell)}, \quad (40)$$

$$\eta^{(\theta)}_{Z^{(i)}}(\ell) = \langle p_+(x,\ell), \psi_{Z^{(i)}}(\cdot,\ell;\theta)\rangle, \quad (41)$$

$$\psi_{Z^{(i)}}(x,\ell;\theta) = \begin{cases} \frac{p_D(x,\ell)p_G g(z_{\theta(\ell)}|x,\ell)}{\kappa(z_{\theta(\ell)})}, & \text{if } \theta(\ell) > 0 \\ q_{D,G}(x,\ell), & \text{if } \theta(\ell) = 0 \end{cases}. \quad (42)$$

and Θ_{I_+} denotes the space of mappings $\theta : I_+ \to \{0,1,...,|Z^{(i)}|\}$, where $\theta(\iota) = \theta(\iota') > 0$ implies $\iota = \iota'$. Since the partitioning of the track labels increases the probability of a missed detection in case of small gates, the gating probability p_G [1] is required in (42) and the missed detection probability is given by $q_{D,G}(x,\ell) = 1 - p_D(x,\ell)p_G$.

In [25], GM and SMC implementations for the required δ-GLMB update are proposed. Since the number of association hypotheses per group increases exponentially in the number of track labels $|\mathbb{L}^{(i)}_+|$, the evaluation of all possible track label to measurement assignments is only feasible for small $|\mathbb{L}^{(i)}_+|$. Similar to the δ-GLMB filter implementation in [24], the posterior distribution (38) is truncated using Murty's algorithm [1], [30] in case of large groups $\mathbb{L}^{(i)}_+$ which facilitates the evaluation of the M most significant hypotheses. Due to the use of target groups, the application of Murty's algorithm which is cubic in complexity, is usually much cheaper than without grouping.

D. Approximation of the updated δ-GLMB as LMB

Finally, the posterior δ-GLMB RFSs for all groups $\mathcal{G}^{(i)}$, $i = 1,...,N$, which are given by (38), have to be approximated by an LMB RFS:

$$\boldsymbol{\pi}^{(i)}(\cdot|Z^{(i)}) \approx \widetilde{\boldsymbol{\pi}}^{(i)}(\cdot|Z^{(i)}) = \left\{\left(r^{(\ell,i)}, p^{(\ell,i)}\right)\right\}_{\ell\in\mathbb{L}^{(i)}_+}.$$

The existence probabilities $r^{(\ell,i)}$ and the spatial distributions $p^{(\ell,i)}$ of each track ℓ are obtained using (26)-(27). Further, the LMB approximation of the full multi-object posterior is given by the union of the approximate LMB groups $\widetilde{\boldsymbol{\pi}}^{(i)}$:

$$\boldsymbol{\pi}(\cdot|Z) \approx \widetilde{\boldsymbol{\pi}}(\cdot|Z) = \bigcup_{i=1}^{N}\left\{\left(r^{(\ell,i)}, p^{(\ell,i)}\right)\right\}_{\ell\in\mathbb{L}^{(i)}_+}. \quad (43)$$

E. Grouping Error

Obviously, the partitioning of the track labels results in a grouping error. In [26], the grouping error is shown to be negligible, i.e.

$$\boldsymbol{\pi}(\mathbf{X}|Z) \approx \boldsymbol{\pi}^{(1)}\left(\widetilde{\mathbf{X}}^{(1)}\,\middle|\,Z^{(1)}\right)\cdots\boldsymbol{\pi}^{(N)}\left(\widetilde{\mathbf{X}}^{(N)}\,\middle|\,Z^{(N)}\right), \quad (44)$$

in case of sufficiently large gating values which coincides with a negligible spatial likelihood of a measurement for a track of another group. For additional details, refer to [26].

F. Track Management

Due to the LMB representation, an intuitive and straightforward track extraction scheme is to select all tracks whose existence probability is higher than a threshold. Obviously, the threshold depends on the application. Further, the track management prunes tracks with an existence probability below an application specific threshold.

V. Results

A. Simulations

The performance of the proposed LMB filter is compared to the multi-Bernoulli filter [6] using the scenario depicted by Figure 2. The filters use a linear constant velocity model with a process noise of $\sigma_a = 5\text{m/s}^2$ and the persistence probability is $p_S = 0.99$. The sensors measures Cartesian x and y positions with a standard deviation of $\sigma = 10m$. The detection probability is $p_D = 0.98$ and the sensor returns a mean number of $\lambda_c = 60$ clutter measurements, which are uniformly distributed over the observation area depicted by Figure 2. The birth model is given by an LMB RFS with four components concentrated at the birth locations.

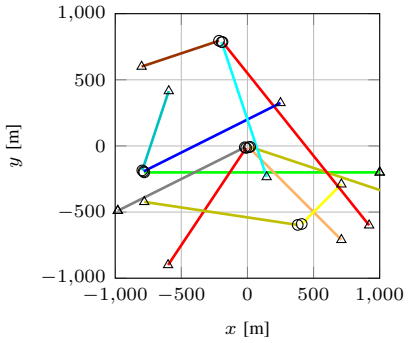

Fig. 2. Ground truth trajectories of the objects. Birth locations marked by a circle, death locations by a triangle.

Figure 3 and Figure 4 show the cardinality estimates and the OSPA distances [31] for the two filters. While the cardinality estimate of the multi-Bernoulli filter is biased, the LMB filter provides accurate cardinality estimates due to the more accurate approximation within the filter update. Due to the cardinality bias, the OSPA distance of the multi-Bernoulli filter is significantly higher than the one of the LMB filter.

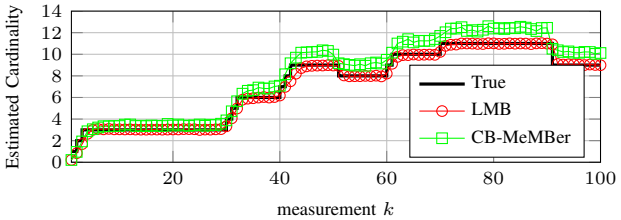

Fig. 3. Cardinality estimates of the LMB and the multi-Bernoulli filter averaged over 100 MC runs.

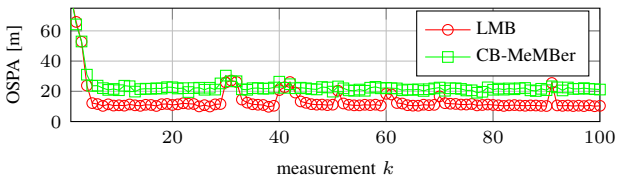

Fig. 4. OSPA distance (cut-off $c = 100$ m, order $p = 1$) of the LMB and the multi-Bernoulli filter averaged over 100 MC runs.

Fig. 5. Snapshot of the tracking results using the LMB filter in an urban scenario: On the left side, the video image and the object hypotheses of the video detector are shown. On the right side, the obtained tracks for the scene are illustrated using green boxes and the black lines represent the trajectories of their motion (relative to the ego vehicle).

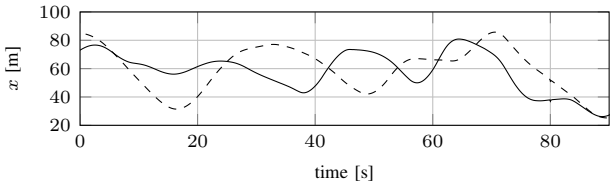

Fig. 6. Distance profile for the two cars performing the overtaking maneuvers.

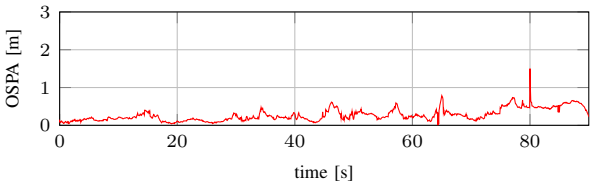

Fig. 7. OSPA distance (cut-off $c = 3$ m, order $p = 1$) of the LMB filter for the scenarios with overtaking maneuvers.

B. Real World Sensor Data

The LMB filter is applied to real world sensor data of our experimental vehicle. The vehicle is equipped with a Continental ARS 308 radar (integrated in the grill), three IBEO Lux laser range finder (integrated in the front bumper), and a video camera (mounted behind the wind-shield). The measurements of the sensors are generated as follows: the radar returns all moving targets using the Doppler measurements, the data of the laser range finders are clustered using a box-fit algorithm [32], and the cascaded classifier presented in [33] is utilized to detect the vehicles in video images. Due to the non-linear motion and measurement models, the equations of the extended Kalman filter are used for linearization.

The accuracy of the filter is evaluated using data of a run on a German highway, where two cars perform overtaking maneuvers. The experimental vehicle and the two other cars are equipped with a differential GPS and an inertial measurement unit to obtain ground truth states. Since the overtaking maneuvers lead to state dependent occlusions, a state dependent detection probability is calculated for each track within a set of track labels I in case of the video and the laser sensor. In contrast, the radar does not require this modeling, since it typically also returns measurements for the occluded car. Figure 6 shows the distance profile for the two cars and Figure 7 shows the OSPA distance for the scenario. Although this scenario is very challenging due to the occlusions, the LMB filter delivers outstanding tracking results.

The LMB filter is also applied to a challenging urban scenario on a busy road. A snapshot of the scenario is given by Figure 5. Since no ground truth data is available for this scenario, an evaluation of the accuracy is not possible. However, the scenario facilitates an evaluation of the real-time capability of the algorithm. Figure 8 depicts the computation times for the LMB filter updates (including prediction) over the complete sequence and Figure 9 illustrates the number of tracked objects. Although the current C++ implementation does not use parallelization, more than 99.9 % of the computation times are below 20 ms and the mean time per filter update is only 2.159 ms. Since the multi-sensor setup delivers 42.5 measurements per second, the average update time is required to be below approx. 23.5 ms. Obviously, there are only a few spikes which exceed the upper bound for the calculation time. Since the spikes are enclosed by updates with a significantly smaller computation time, the proposed LMB filter is real-time capable for the investigated scenario.

VI. Conclusion

The labeled multi-Bernoulli filter proposed in this contribution is a tractable and efficient multi-object tracking algorithm which approximates the multi-object posterior distribution using a labeled multi-Bernoulli RFS. The filter inherits the intuitive track representation of the multi-Bernoulli filter as well as the accurate measurement update of the δ-generalized labeled multi-Bernoulli filter. Further, the filter does not exhibit the cardinality bias of the multi-Bernoulli filter and the exponentially increasing number of components of the δ-GLMB filter. The structure of the filter facilitates parallelization since the prediction of the individual tracks as well as group based

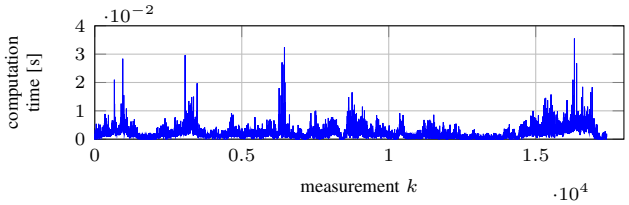

Fig. 8. Computation times of the LMB filter update for the urban scenario.

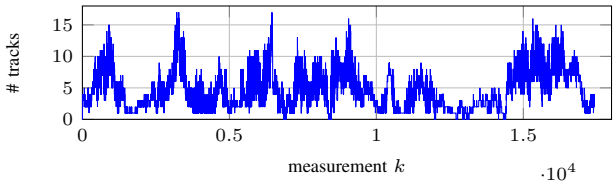

Fig. 9. Number of tracks (including birth tracks) for the urban scenario.

measurement updates are independent. The simulation results illustrate the possible performance gain compared to the multi-Bernoulli filter. Further, the results using the multi-sensor setup of the experimental vehicle indicate the real-time capability of the proposed labeled multi-Bernoulli filter.

ACKNOWLEDGEMENT

This work is supported by the German Research Foundation (DFG) within the Transregional Collaborative Research Center SFB/TRR 62 "Companion-Technology for Cognitive Technical Systems" and by the Australian Research Council under schemes DE120102388 and FT0991854.

REFERENCES

[1] S. Blackman and R. Popoli, *Design and Analysis of Modern Tracking Systems*. Artech House Publishers, 1999.

[2] Y. Bar-Shalom and T. Fortmann, *Tracking and Data Association*. Academic Press, Inc., 1988.

[3] R. Mahler, *Statistical Multisource-Multitarget Information Fusion*. Artech House Inc., Norwood, 2007.

[4] ——, "Multitarget Bayes filtering via first-order multitarget moments," *IEEE Transactions on Aerospace and Electronic Systems*, vol. 39, no. 4, pp. 1152–1178, 10 2003.

[5] ——, "PHD filters of higher order in target number," *IEEE Transactions on Aerospace and Electronic Systems*, vol. 43, no. 4, pp. 1523–1543, 10 2007.

[6] B.-T. Vo, B.-N. Vo, and A. Cantoni, "The cardinality balanced multi-target multi-Bernoulli filter and its implementations," *IEEE Transactions on Signal Processing*, vol. 57, no. 2, pp. 409–423, 2 2009.

[7] B.-N. Vo, B.-T. Vo, N.-T. Pham, and D. Suter, "Joint detection and estimation of multiple objects from image observations," *IEEE Transactions on Signal Processing*, vol. 58, no. 10, pp. 5129–5141, 2010.

[8] B.-N. Vo, S. Singh, and A. Doucet, "Sequential Monte Carlo methods for multitarget filtering with random finite sets," *IEEE Transactions on Aerospace and Electronic Systems*, vol. 41, Issue 4, pp. 1224–1245, 2005.

[9] H. Sidenbladh and S.-L. Wirkander, "Tracking random sets of vehicles in terrain," in *Conference on Computer Vision and Pattern Recognition Workshop*, 2003, p. 98.

[10] T. Zajic and R. Mahler, "A particle-systems implementation of the PHD multitarget-tracking filter," in *Signal Processing, Sensor Fusion, and Target Recognition XII, SPIE, Vol. 5096*, Bellingham, WA, 2003, pp. 291–299.

[11] B.-N. Vo and W.-K. Ma, "The Gaussian mixture probability hypothesis density filter," *IEEE Transactions on Signal Processing*, vol. 54, no. 11, pp. 4091–4104, 11 2006.

[12] B.-T. Vo, B.-N. Vo, and A. Cantoni, "Analytic implementations of the cardinalized probability hypothesis density filter," *IEEE Transactions on Signal Processing*, vol. 55, no. 7, pp. 3553–3567, 7 2007.

[13] J. J. Yin and J. Q. Zhang, "The nonlinear multi-target multi-Bernoulli filter using polynomial interpolation," in *IEEE 10th International Conference on Signal Processing (ICSP)*, 2010, pp. 2551–2554.

[14] C. Ouyang, H. Ji, and C. Li, "Improved multi-target multi-Bernoulli filter," *IET Radar, Sonar and Navigation*, vol. 6, no. 6, pp. 458–464, 2012.

[15] V. Ravindra, L. Svensson, L. Hammarstrand, and M. Morelande, "A cardinality preserving multitarget multi-Bernoulli RFS tracker," in *Information Fusion (FUSION), 2012 15th International Conference on*, 2012, pp. 832–839.

[16] B.-T. Vo, B.-N. Vo, R. Hoseinnezhad, and R. Mahler, "Robust multi-Bernoulli filtering," *IEEE Journal of Selected Topics in Signal Processing*, vol. 7, no. 3, pp. 399–409, 2013.

[17] R. Hoseinnezhad, B.-N. Vo, B.-T. Vo, and D. Suter, "Visual tracking of numerous targets via multi-Bernoulli filtering of image data," *Pattern Recognition*, vol. 45, no. 10, pp. 3625–3635, 2012.

[18] R. Hoseinnezhad, B.-N. Vo, and B.-T. Vo, "Visual tracking in background subtracted image sequences via multi-Bernoulli filtering," *IEEE Transactions on Signal Processing*, vol. 61, no. 2, pp. 392–397, 2013.

[19] X. Zhang, "Adaptive control and reconfiguration of mobile wireless sensor networks for dynamic multi-target tracking," *IEEE Transactions on Automatic Control*, vol. 56, no. 10, pp. 2429–2444, 2011.

[20] J. Lee and K. Yao, "Initialization of multi-Bernoulli random-finite-sets over a sensor tree," in *International Conference on Acoustics, Speech and Signal Processing (ICASSP)*, 2012.

[21] R. Hoseinnezhad, B.-N. Vo, B.-T. Vo, and D. Suter, "Bayesian integration of audio and visual information for multi-target tracking using a CB-MeMBer filter," in *IEEE International Conference on Acoustics, Speech and Signal Processing (ICASSP)*, 2011, pp. 2300–2303.

[22] J. Williams, "Hybrid Poisson and multi-Bernoulli filters," in *Information Fusion (FUSION), 2012 15th International Conference on*, 2012, pp. 1103–1110.

[23] B.-T. Vo and B.-N. Vo, "A random finite set conjugate prior and application to multi-target tracking," in *Proceedings of the 7th International Conference on Intelligent Sensors, Sensor Networks and Information Processing*, 12 2011, pp. 431–436.

[24] ——, "Labeled random finite sets and multi-object conjugate priors," *IEEE Transactions on Signal Processing*, vol. 61, no. 13, pp. 3460–3475, 2013.

[25] B.-N. Vo, B.-T. Vo, and D. Phung, "Labeled random finite sets and the bayes multi-target tracking filter," *pre-print*, 2013. [Online]. Available: http://arxiv.org/abs/1312.2372

[26] S. Reuter, B.-T. Vo, B.-N. Vo, and K. Dietmayer, "The labeled multi-Bernoulli filter," *IEEE Transactions on Signal Processing*, vol. 62, no. 12, pp. 3246 – 3260, 2014.

[27] J. Dezert and Y. Bar-Shalom, "Joint probabilistic data association for autonomous navigation," *IEEE Transactions on Aerospace and Electronic Systems*, vol. 29, no. 4, pp. 1275–1286, 10 1993.

[28] D. Eppstein, "Finding the k shortest paths," *SIAM Journal on Computing*, vol. 28, no. 2, pp. 652–673, 1998.

[29] J. Y. Yen, "Finding the k shortest loopless paths in a network," *Management Science*, vol. 17, no. 11, pp. 712–716, 07 1971.

[30] K. Murty, "An algorithm for ranking all the assignments in order of increasing cost," *Operations Research*, vol. 16, pp. 682–687, 1968.

[31] D. Schuhmacher, B.-T. Vo, and B.-N. Vo, "A consistent metric for performance evaluation of multi-object filters," *IEEE Transactions on Signal Processing*, vol. 56, no. 8, pp. 3447–3457, 8 2008.

[32] M. Munz, "Generisches Sensorfusionsframework zur gleichzeitigen Zustands- und Existenzschätzung für die Fahrzeugumfelderkennung," Ph.D. dissertation, Ulm University, 7 2011.

[33] M. Gabb, O. Löhlein, R. Wagner, A. Westenberger, M. Fritzsche, and K. Dietmayer, "High-performance on-road vehicle detection in monocular images," in *Proceedings of the 16th International IEEE Conference on Intelligent Transportation Systems*, 2013, pp. 336–341.